Distortion Analysis of 1.3 µm AlGaInAs/InP Transistor Laser

R. Ranjith, S. Piramasubramanian and M. Ganesh Madhan

Abstract We analyze the distortion characteristics of 1.3 µm AlGaInAs/InP Transistor Laser for CATV applications. The characteristics of Transistor Laser are analyzed by solving rate equations. Small signal analysis has been done for different input bias currents. Bandwidth and resonance frequency are calculated from the small signal analysis. Second harmonic distortion (2HD) is evaluated for different input bias currents. Third order intermodulation distortion (IMD3) is calculated with two input frequencies of 823.25 and 815.25 MHz. Minimum 2HD of −20.76 dBc and IMD3 of −33.61 dBc are predicted from this study.

1 Introduction

Optical communication is one of the key technologies to provide high bandwidth to users. However, optical sources such as laser diode is capable of providing only an intrinsic bandwidth up to 40 GHz [1]. So there is a need for alternate device to provide bandwidth in excess of 40 GHz. Transistor Laser (TL) operates at 980 nm was invented by Feng et al. [2, 3]. The TL is a transistor with quantum wells in its base. Quantum well in active region provides laser light output. Charge control analysis of the TL was reported by Feng et al. [4]. Electrons emitted from the emitter terminal is captured by the quantum well region because of its lower bandgap (heterostructure) with a capture time of t_{cap} and the uncaptured electrons are captured by collector terminal due to reverse bias. This reduces the carrier lifetime and increases the bandwidth when compared with conventional laser

R. Ranjith (✉) · S. Piramasubramanian · M. Ganesh Madhan
Department of Electronics Engineering, Madras Institute of Technology Campus, Anna University, Chennai, India
e-mail: ranjith4792@gmail.com

S. Piramasubramanian
e-mail: spsnanthan@gmail.com

M. Ganesh Madhan
e-mail: mganesh@annauniv.edu

I. Bhattacharya et al. (eds.), *Advances in Optical Science and Engineering*, Springer Proceedings in Physics 194, DOI 10.1007/978-981-10-3908-9_52

diodes. The dynamic operation of TL has been modeled to a coupled rate equations for numerical analysis by Zhang and Leburton [5] and Faraji et al. [6–8]. The wavelengths used in the conventional optical communication system are 1.5 and 1.3 μm, due to low attenuation and dispersion in fiber respectively. An 1.3 μm AlGaInAs/InP TL was designed and demonstrated at room temperature by Shirao et al. [9]. The operation and experiments of the TL in CE and CB configuration with charge control analysis was investigated by Feng et al. [9–13]. In this work, we analyze the distortion characteristics of TL at 823.25 and 815.25 MHz. The second order harmonics and third order intermodulation products are observed and calculated for different base currents.

2 Modeling of Transistor Laser

AlGaInAs/InP TL is represented by coupled rate equations developed by Faraji et al. [6] for numerical analysis and the large signal analysis was done by Shirao et al. [9]. The charge control model is given in Fig. 1, the excess carriers flow from the emitter terminal to the collector terminal is captured by the quantum well, which is placed in the middle of the base region, with width of d (nm). The emitter and collector current in Fig. 1 flows in the direction opposite that of electron flow.

The transistor laser rate equations used for numerical analysis are given below [9].

$$\frac{dN_{vs}}{dt} = -\frac{N_{vs}}{\tau_{cap}} - \frac{N_{QW}}{\tau_{esc}} + \frac{Ivs}{dqA} \tag{1}$$

$$\frac{dN_{QW}}{dt} = \frac{N_{vs}}{\tau_{cap}} - \frac{N_{QW}}{\tau_{esc}} - \frac{g's\left(N_{QW} - N_g\right)}{1 + \epsilon_{\text{other}} s} - \frac{N_{QW}}{\tau_s} \tag{2}$$

$$\frac{dS}{dt} = \frac{\epsilon G' S\left(N_{QW} - N_g\right)}{1 + \epsilon_{\text{other}} S} - \frac{S}{\tau_p} + C\frac{N_{QW}}{\tau_s} \tag{3}$$

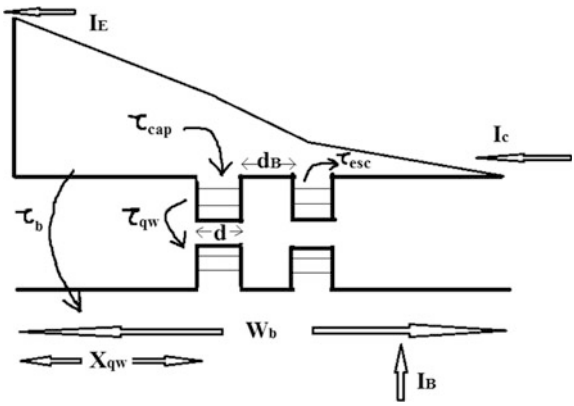

Fig. 1 Charge concentration in base region in two quantum well transistor laser [5]

Equation (1) denotes the virtual state carrier density of the region above the quantum well. I_{vs} is the current available in the higher energy state region above the QW [9]. Equation (2) represents the QW carrier density. The photon density extracted from the QW is provided in (3). The parameters used in the above coupled rate equations for 1.3 μm AlGaInAs/InP TL has been taken from Shirao et al. [9]. The above equations are numerically solved by using MATLAB®. Optical power output from the TL is formulated by the (4) [12].

$$P = \eta\, v_g(\alpha_i + \alpha_m) h\, f\, S\, (v/2\epsilon) \tag{4}$$

where v is active layer volume and v_g is the group velocity. Based on the charge continuity equation, the penetration of minority carrier in the device depends on input frequency i.e. diffusion length [9].

$$L_D = \sqrt{\frac{D_n \tau_b}{1 + j\omega\tau_b}} \quad L_D = \sqrt{D_n \tau_b} \tag{5}$$

From (5) the diffusion length is inversely proportional to the given frequency. For DC characteristics diffusion length is defined by taking $\omega = 0$.

3 Simulation Results

3.1 DC Characteristics

The DC characteristics of a transistor laser have been analyzed by giving a constant bias current as input. NPN TL is made to work in the active region by forward biasing the base emitter junction and reverse biasing the base collector junction. The coupled rate equations are solved by keeping time derivatives equal to zero. The threshold current is calculated by plotting optical power for different input DC currents. Optical power is calculated from (4) and plotted in Fig. 2. The estimated

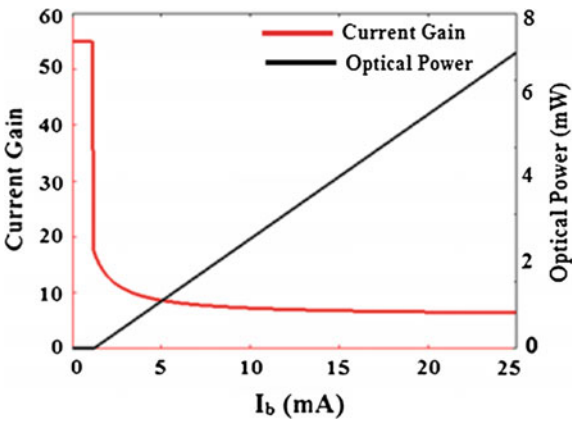

Fig. 2 Optical power and current gain variation with base current

threshold base current for two quantum well transistor laser from Fig. 2 is 1 mA. Before the threshold current, only spontaneous emission occurs. The stimulated emission is made possible by achieving population inversion by increasing the input current. The current gain β is represented in Fig. 2. It is found that the current gain decreases drastically beyond threshold current. This is due to high recombination in the base region which includes quantum well.

3.2 Small Signal Analysis

Small signal analysis is done by choosing different bias input currents after threshold and by giving input AC signal within the chosen linear region in the nonlinear transfer characteristics of TL [1].

$$I(t) = I_b + I_m \sin(\omega t) \tag{6}$$

where, I_b is the bias current and I_m is the amplitude of the time varying input signal. By varying the input current below and above the threshold, the output optical power also varies, which is called direct or intensity modulation. Increasing the frequency also the limits the performance due to the rate of depletion of stored minority carriers. Magnitude response versus frequency was determined for different input bias currents. The magnitude plot for different input bias currents are shown in Fig. 3a. From Fig. 3 it is found that the bandwidth and resonance frequency increases for increasing the input base current. From Fig. 3b the bandwidth achieved by TL in CE configuration is found as 40 GHz when the bias current is fixed as 200 mA ($200I_{th}$). Hence it is clear that direct modulation by using TL can reach up to 40 GHz bandwidth which is not the case in laser diodes. However, the bandwidth saturates at 40 GHz, even with increasing base current.

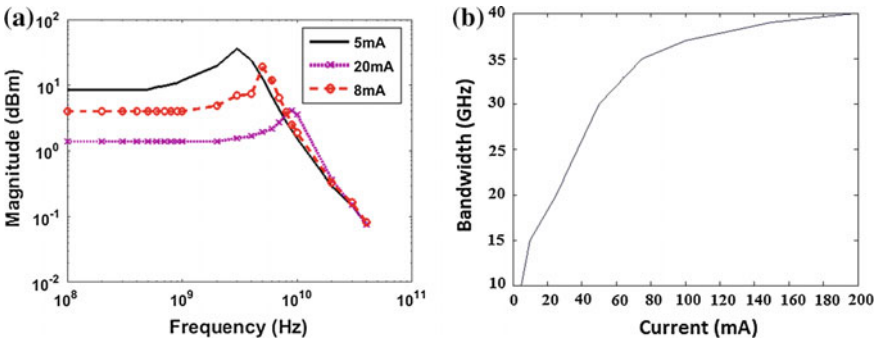

Fig. 3 **a** Magnitude response and **b** bandwidth variation with bias current

3.3 *Harmonic Analysis*

Due to non linear characteristics of the TL, the harmonics other than the fundamental component also generated. Hence an analysis of harmonics developed by the TL becomes necessary. Harmonic analysis is carried out to predict second harmonic distortion and third order intermodulation distortion. These distortion have to be reduced in analog optical link and RoF applications [13].

3.3.1 Second Order Harmonic Distortion

An 823.25 MHz signal (CH 65 of video carrier in CATV Band) is given as input to the TL. The given AC signal, intensity modulate with the optical carrier. FFT of the output optical signal is taken by 524,288 sampling points to plot the frequency spectrum of the input signal. The spectrum of input signal and corresponding optical power are shown in Fig. 4a, b respectively. The input signal spectrum is plotted in Fig. 4a with fundamental component at 823.25 MHz with magnitude of 4.22 dBm. Due to the nonlinear characteristics of the TL, the output spectrum has

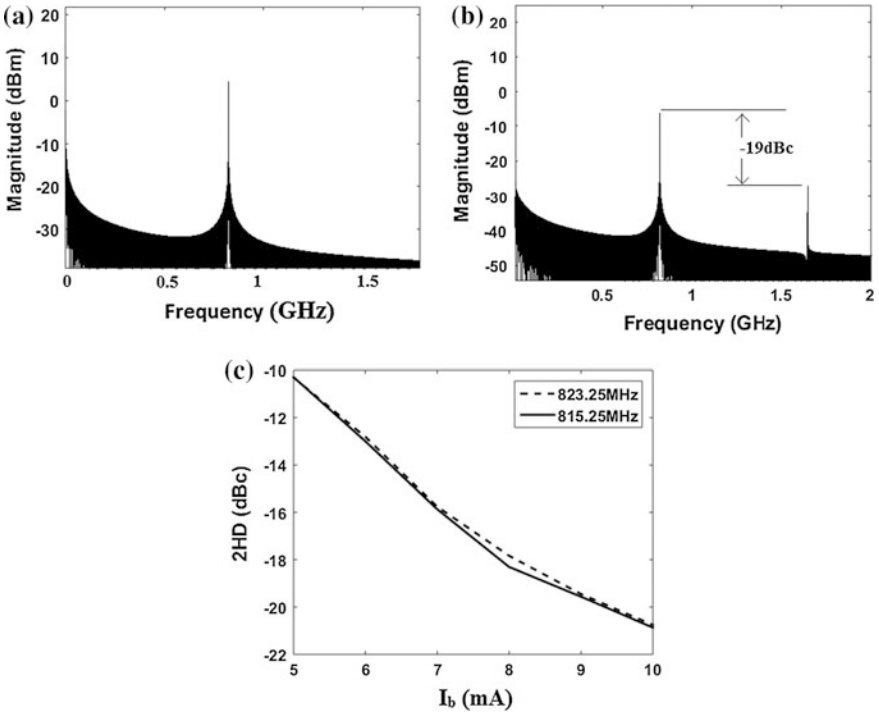

Fig. 4 **a** Spectrum of current at 823.25 MHz **b** spectrum of optical power and **c** variation of 2HD with bias current

additional harmonic components than the required fundamental one. From the small signal analysis, it has been found that the device bandwidth increases with increasing bias current. Hence the effect of bias current in second harmonic distortion (2HD) is also determined and shown in Fig. 4c. The 2HD is measured in (dBc), which is the difference between the fundamental one and the second harmonic component. As the input bias current increases, the 2HD decreases (Fig. 4c). A minimum of −21 dBc is observed for the bias current of 10 mA.

3.3.2 Third Order Intermodulation Distortion (IMD3)

In applications such as Radio over Fiber (ROF), the input signal has more than one frequency component. For simplicity we consider an input signal which contains two tones. The intermodulated harmonic components occur more closely to the fundamental frequency, than the second order harmonics [13]. For CATV applications IMD products are analyzed within the 8 MHz span of the video carrier. We have chosen two video carriers 815.25 and 823.25 MHz (CH 64 and CH 65) and the input and output spectrum are plotted in Fig. 5a, b. It has been observed that the

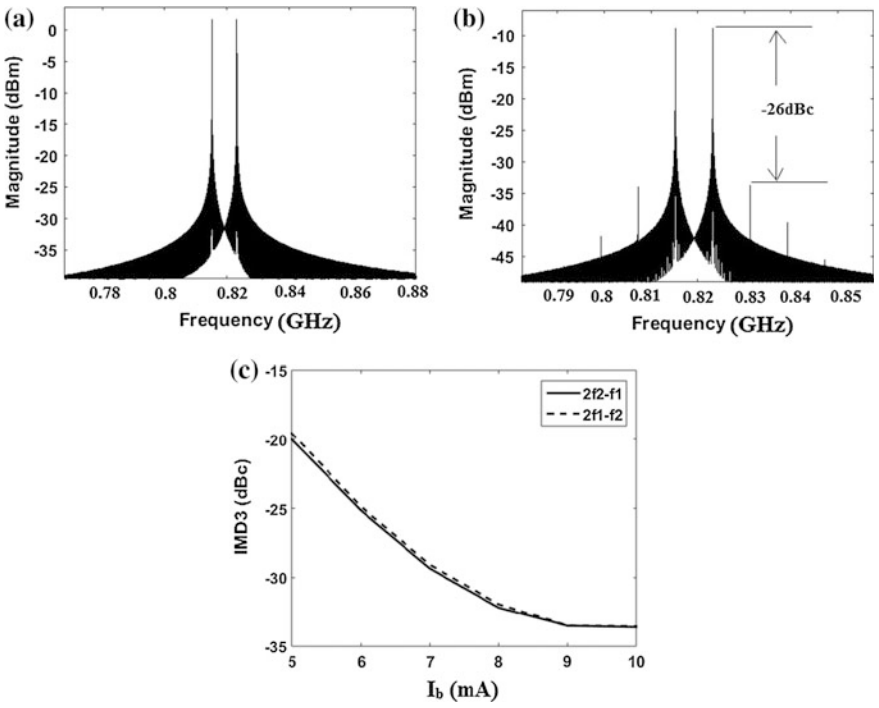

Fig. 5 **a** Spectrum of two tone input signal at f_1 = 815.25 MHz and f_2 = 823.25 MHz **b** spectrum of optical power and **c** variation of IMD3 with bias current

output has additional frequency components compared to the input. The variation of IMD3 with bias current in shown in Fig. 5c.

From this analysis, it has been found that the third order intermodulation component occurs more closely to the fundamental tone within 8 MHz span of the video carrier. The other intermodulated components closer to the fundamental tone are fifth and seventh order components. It also found that the IMD3 components have large magnitude than other IMD products. The IMD3 for different input bias currents has been calculated to study the effect of input bias current. The IMD3 products are found to decrease for increasing input bias currents and a minimum of −33.61 dBc is predicted for a bias current of 10 mA.

4 Conclusion

The DC and AC characteristics of transistor laser are analyzed by numerically solving rate equations. It has been found that the bandwidth increases for increasing the input bias current and a maximum bandwidth of 40 GHz is predicted. The second harmonic distortion and third order intermodulation distortion are analyzed for different base currents. The distortion of TL decreases with increasing the input bias currents. A minimum 2HD of −20.76 dBc and IMD3 of −33.61 dBc are predicted in our analysis for the bias current of 10 mA.

References

1. Gerd keiser, “Optical Fiber Communications” Special Indian Edition McGraw Hill (2013).
2. G. Walter, Nick Holonyak Jr., M. Feng and R. Chan, “Laser Operation of a Heterojunction Bipolar Light Emitting Transistor”, Applied Physics Letters, 85, 4768 (2004).
3. M. Feng, N. Holonyak Jr., G. Walter, and R. Chan, “Room temperature continuous wave operation of a heterojunction bipolar transistor laser”, Applied Physics letters 87, 131103 (2005).
4. M. Feng, N. Holonyak Jr., H. W. Then, and G. Walter, “Charge control analysis of transistor laser operation”, Applied Physics letter 91, 053501 (2007).
5. Lingxiao Zhang,, and Jean-Pierre Leburton, “Modeling of the Transient Characteristics of Heterojunction Bipolar Transistor Lasers”, IEEE Quantum Electronics, Vol 45, No. 4, (2009).
6. B. Faraji, D. L. Pulfrey, and L. Chrostowski, “Small-signal modeling of the transistor laser including the quantum capture and escape lifetimes”, Applied Physics letters 93, 103509 (2008).
7. B. Faraji, W. Shi, D. L. Pulfrey, and L. Chrostowski. “Common-emitter and common-base small-signal operation of the transistor laser”, Applied Physics letters 93, 143508 (2008).
8. Behnam Faraji, Wei Shi, David L. Pulfrey, and Lukas Chrostowski “Analytical Modeling of the Transistor Laser”, IEEE Journal of selected topics in Quantum Electonics, Vol 5, No 3. (2009).
9. Mizuki Shirao, Masashi, Seunghun Lee, Nobuhiko Nishiyama, and Shigehisa Arai, “Large Signal Analysis of Transistor Laser” IEEE Quantum Electronics Vol. 47, No. 3, (2011).

10. Mizuki Shirao, Takashi Sato, Noriaki Sato, Nobuhiko Nishiyama, and Shigehisarai, “Room-temperature operation of npn-AlGaInAs/InP multiple quantum well transistor laser emitting at 1.3-μm wavelength”, OSA OPTICS EXPRESS Vol 20, No 4, (2012).
11. Larry A. Coldren, “Diode Lasers and Photonic Integrated Circuits”, Wiley Series in Microwave and Optical Engineering (2012).
12. S. Piramasubramanian, M. Ganesh Madhan, Jyothsna Nagella, G. Dhanapriya, ‘Numerical analysis of distortion characteristics of heterojunction bipolar transistor laser’, Optics Communications 357, 177–184 (2015).
13. Safwat W. Z. Mahmood, Alaa Mahmood and Mousatfa Ahmed, “Noise Performance and nonlinear distortion of semiconductor laser under two tone modulation for use in analog CATV systems”, International Journal Of Numerical Modelling: Electronic Networks, Devices And Fields, Int. J. Numer. Model (2015).